JACS
JOURNAL OF THE AMERICAN CHEMICAL SOCIETY
Article
pubs.acs.org/JACS

Hiding and Recovering Electrons in a Dimetallic Endohedral Fullerene: Air-Stable Products from Radical Additions

Michio Yamada,[†] Hiroki Kurihara,[‡] Mitsuaki Suzuki,[‡] Masayoshi Saito,[‡] Zdenek Slanina,[‡] Filip Uhlik,[§] Toshihiro Aizawa,[∥] Tatsuhisa Kato,[∥,⊥] Marilyn M. Olmstead,[#] Alan L. Balch,[#] Yutaka Maeda,[†] Shigeru Nagase,[▽] Xing Lu,[○] and Takeshi Akasaka*[,†,‡,○,◆]

[†]Department of Chemistry, Tokyo Gakugei University, Tokyo 184-8501, Japan
[‡]Life Science Center of Tsukuba Advanced Research Alliance, University of Tsukuba, Tsukuba, Ibaraki 305-8577, Japan
[§]Department of Physical and Macromolecular Chemistry, Charles University in Prague, 128 43 Prague 2, Czech Republic
[∥]Graduate School of Human and Environmental Sciences and [⊥]Institute for Liberal Arts and Sciences, Kyoto University, Kyoto 606-8501, Japan
[#]Department of Chemistry, University of California Davis, Davis, California 95616, United States
[▽]Fukui Institute for Fundamental Chemistry, Kyoto University, Kyoto 606-8103, Japan
[○]College of Materials Science and Engineering, Huazhong University of Science and Technology 430074 Wuhan, China
[◆]Foundation for Advancement of International Science, Tsukuba, Ibaraki 305-0821, Japan

Supporting Information

ABSTRACT: Fullerenyl radicals can be generated by addition of a free radical to a fullerene surface, by nucleophilic addition followed by one-electron oxidation, or by thermal dissociation of singly bonded fullerene dimers. However, fullerenyl radicals are usually very reactive and generally cannot be isolated. On the contrary, we have found that the reactions of the dimetallic endofullerenes, $La_2@I_h$-C_{80} and $La_2@D_{5h}$-C_{80}, with 3-chloro-5,6-diphenyltriazine resulted in mono-addition of the triazinyl radical to the fullerene cages to yield isolable fullerenyl radicals. The unusual stability of these fullerenyl radicals arises from the confinement of the unpaired electron to an internal, metal−metal bonding orbital. Accordingly, the fullerene cage protects the radical center from other reactive species. Furthermore, we demonstrate that the fullerenyl radical adduct of $La_2@I_h$-C_{80} reacts with toluene to afford additional benzylation. Interestingly, the benzylated derivative is diamagnetic in solution, while it forms a paramagnetic dimer when crystallized.

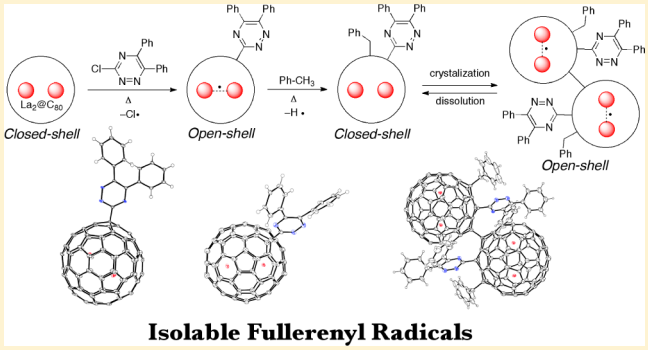

INTRODUCTION

Neutral free radicals are fundamentally important chemical species that are useful for applications in polymer chemistry, materials science, and biochemistry.[1] Fullerenes exhibit high radical scavenging activity by virtue of their high electron affinity and the large number of conjugated double bonds that can be readily attacked by free radicals.[2,3] Monoaddition of a radical to C_{60} yields fullerenyl radicals ($R-C_{60}\bullet$).[4−11] Alternatively, fullerenyl radicals can be generated by nucleophilic addition and subsequent one-electron oxidation or by thermal dissociation of singly bonded fullerene dimers. However, such fullerenyl radicals are usually very reactive and cannot be isolated. EPR studies of C_{60}-based fullerenyl radicals showed that an unpaired electron was not delocalized over the C_{60} surface but rather confined to the carbon atom ortho and the two carbon atoms para to the point of attachment of the addend. Nevertheless, fullerene-based neutral radicals can be considered to be intriguing candidates for photoactive materials in organic photovoltaics (OPVs).[12,13] Indeed, C_{60} and its derivatives are known to exhibit excellent performance in donor−acceptor heterojunction-type OPVs.[14] In this respect, Nakamura et al. have recently demonstrated that thermal treatment of a solid fullerene dimer ($R-C_{60}-C_{60}-R$) resulted in generation of a long-lived fullerenyl radical intermediate ($R-C_{60}\bullet$), which led to an increase in the electron mobility of the solid.[15] The relatively long lifetime of the fullerenyl radical intermediate is attributable to the plastic nature of these fullerene crystals.

Encapsulation of metal atoms in fullerene cages can result in electronic configurations that are more complex than those of empty fullerenes.[16−18] For example, dimetallic endofullerenes, such as $La_2@I_h$-C_{80}, exhibit endohedral redox activity, in which the encaged La atoms act as the reduction-active species,

Received: September 26, 2014
Published: December 10, 2014

DOI: 10.1021/ja509956y
J. Am. Chem. Soc. 2015, 137, 232−238

whereas the fullerene cage scarcely takes part in the reduction process.[19] In fact, the LUMO of $La_2@I_h$-C_{80} is associated with the La–La σ-bonding orbital, whereas the HOMO and other occupied molecular orbitals (MOs) near HOMO are distributed over the carbon cage.[20,21] Consequently, an unpaired electron could be confined to the internal La atoms rather than delocalized onto the fullerene cage when $La_2@I_h$-C_{80} is reduced under chemical or electrochemical conditions.[22,23] This type of electron uptake is known as an endohedral electron-transfer process, though it is not known whether such electron transfer occurs through the intermediate state with the charge localized on the fullerene cage or whether the electron tunnels through the fullerene cage. We consider that such an internal LUMO could stabilize fullerenyl radicals.

In this article, we report the first example of an isolable fullerenyl radical, synthesized by the thermal reaction of $La_2@I_h$-C_{80} with 3-chloro-5,6-diphenyltriazine. The extraordinary stability of the fullerenyl radical is due to confinement of the unpaired electron to the isolated La–La σ-bonding orbital inside the fullerene cage. Similar reactivity was also found in a second isomer of $La_2@C_{80}$, $La_2@D_{5h}$-C_{80}. The corresponding radical was successfully isolated and characterized. Additionally, the reactivity of the fullerenyl radical of $La_2@I_h$-C_{80} toward toluene and the unusual dimerization/dissociation character of the resulting benzylated derivative were investigated, as described below.

RESULTS AND DISCUSSION

Reaction of $La_2@I_h$-C_{80} with 3-Chloro-5,6-diphenyltriazine. A 1,2-dichlorobenzene (1,2-DCB) solution containing $La_2@I_h$-C_{80} and an excess amount of 3-chloro-5,6-diphenyltriazine (**1**) was heated under reflux for 24 h (Figure 1). The mixture was analyzed using analytical high-performance

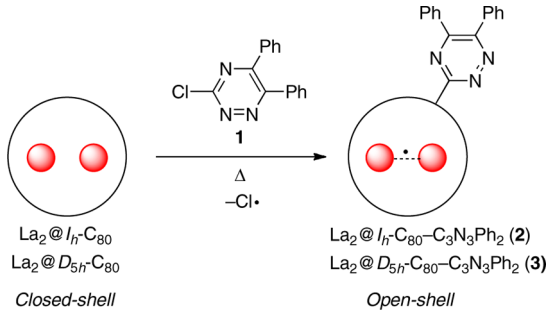

Figure 1. Reactions of $La_2@C_{80}$s with **1**.

liquid chromatography (HPLC), and a single new peak was observed. The product (**2**) was easily isolated by preparative HPLC using a Buckyprep column. The matrix-assisted laser desorption ionization–time-of-flight (MALDI–TOF) mass spectrometry of isolated **2** showed a strong peak at m/z 1470, suggesting that **2** consists of a radical coupled product of triazinyl radical with $La_2@I_h$-C_{80} (i.e., $La_2@I_h$-C_{80}–$C_3N_3Ph_2$). Moreover, this radical **2** is stable in air. The analytical HPLC and mass spectrometric analyses revealed that further coupling of **2** with other radicals did not proceed under our experimental conditions.

There are only two nonequivalent carbon atoms in the I_h-C_{80} cage, named [5,6,6]- and [6,6,6]-carbon atoms; the former is shared by one pentagon and two hexagon rings, and the latter is shared by three hexagon rings. The position of addition in **2** was determined using single-crystal X-ray diffraction (XRD). The structure shown in Figure 2 confirms that the addition of

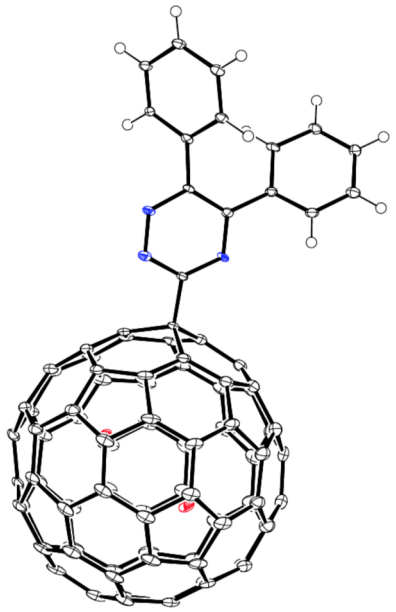

Figure 2. ORTEP drawing of **2** and with thermal ellipsoids shown at the 50% probability level for 90 K. Solvate molecules are omitted for clarity. Only the major lanthanum sites and the major cage orientation are shown.

the carbon-centered triazinyl radical took place at one of the [5,6,6]-carbon atoms. The crystal displays some disorder. There are two overlapping orientations of the cage with refined occupancies of 0.79 and 0.21. The cage disorder comes from rotation along the single bond to the triazinyl group. The lanthanum atoms are also subject to disorder. There is one prominent La pair with 0.67–0.69 site-occupancy. Twelve additional sites have been identified with occupancies ranging from 0.03 to 0.10.

The electronic absorption spectrum of **2** exhibits broad absorption bands over the near-IR region down to 1300 nm (Figure 3a). As a consequence of the paramagnetic nature in **2**,

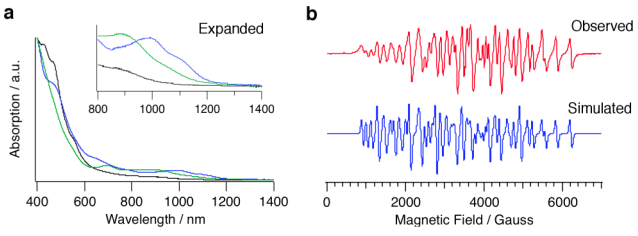

Figure 3. (a) Electronic absorption spectra of $La_2@I_h$-C_{80} (black line), **2** (blue line), and **4** (green line) in CS_2. (b) Observed (red line) and simulated (blue line) X-band EPR spectra of **2** in CS_2 observed at room temperature.

no meaningful NMR spectra were observed. The paramagnetic character of **2** was confirmed by X-band EPR measurements. As illustrated in Figure 3b, the EPR signal of **2** resembles that of $La_2@I_h$-C_{80} anion radical. In this context, the electronic structure of **2** can be formally described as $(La_2)^{5+}(I_h\text{-}C_{80}\text{–}C_3N_3Ph_2)^{6-}$. The unpaired electron, formed by the radical coupling process, is not distributed on the carbon cage but is confined to the internal, La–La σ-bonding orbital. The

DOI: 10.1021/ja509956y
J. Am. Chem. Soc. 2015, 137, 232–238

observed spectrum is well reproduced by the simulation using the parameters: $S = 1/2$, $g = 1.899$, $A(La_1) = A(La_2) = 35.9$ mT, $\Delta H_{pp} = 7$ mT. The simulation reveals two important observations: one, a large spin density is associated with each La atom; two, each La atom has the same spin density. Although the two La atoms are found at inequivalent sites in the X-ray structure, the rotation of the La ions within the cage can readily average out the spin density during the time scale of EPR spectroscopy. To rationalize the assumption of averaging by the rotation of La ions, we refer to the result of ESR measurement of $La_2@C_{80}$ anion radical, see Figures S19–S22. The spectrum of **2** was similar to that of $La_2@C_{80}$ anion radical at 180 K. The equally spaced hyperfine structure at the higher magnetic field never fits the simulation without using the isotropic parameters of $A(La_1) = A(La_2) = 35.9$ mT.

The redox potentials of **2** were investigated using cyclic (CV) and differential pulse voltammetry (DPV) measurements (see Figure S5 and Table S1). The fullerenyl radical **2** exhibited two reversible reduction processes and one reversible oxidation process followed by an irreversible oxidation process. Compared with those of $La_2@I_h$-C_{80}, the first reduction potential of **2** was shifted cathodically by 430 mV, whereas the first oxidation potential of **2** was shifted cathodically by 410 mV.

To gain deeper insight into the formation and the electronic properties of **2**, density functional theory (DFT) calculations were conducted at the B3LYP/6-31G(d) ~ sdd level. As shown in Figure S6, the SOMO of **2** is associated with the internal La–La σ-bonding orbital, as found in the case of $La_2@I_h$-C_{80} anion radical.[23] The spin densities on the La atoms were calculated to be 0.487 and 0.469, showing that the unpaired electron was not distributed to the carbon cage but rather localized on the internal La atoms. Energy diagrams of $La_2@I_h$-C_{80} anion radical and **2** are depicted in Figure S17. The SOMO (α-HOMO) of **2** (−4.74 eV) is much lower in energy than that of $La_2@I_h$-C_{80} anion radical (−2.06 eV). The results also support the unusual chemical stability of **2**.

One can consider the other possible isomer, in which the triazinyl radical is connected to one of the [6,6,6]-carbon atoms. However, the DFT calculations reveal that the [6,6,6]-adduct is 8.51 kcal mol^{-1} higher in energy than the [5,6,6]-adduct. Therefore, thermodynamic considerations probably control the regioselective formation of **2**. Interestingly, the SOMO of the [6,6,6]-adduct is delocalized not only on the La atoms but also on the carbon cage (see Figure S6). In this context, the [6,6,6]-adduct could also be kinetically unstable. Overall, the results indicate that the unpaired electron is confined to the internal La–La σ-bonding orbital where it is protected from external attack by the diamagnetic carbon cage.[24]

Reaction of $La_2@D_{5h}$-C_{80} with 3-Chloro-5,6-diphenyl-triazine. The second isomer of $La_2@C_{80}$, $La_2@D_{5h}$-C_{80}, was first reported in 1997.[25] However, the much lower yield of $La_2@D_{5h}$-C_{80} compared with that of $La_2@I_h$-C_{80} has inhibited the study of its properties. In this study, we succeeded in the preparation of a sufficient amount of $La_2@D_{5h}$-C_{80} to examine its structure and reactivity. The I_h-C_{80} and D_{5h}-C_{80} cages have very similar structures. If one cuts the D_{5h}-C_{80} cage along the horizontal mirror plane, rotates the top half by 36°, and reattaches the top to the bottom, the I_h-C_{80} cage is obtained. The D_{5h}-C_{80} cage has six different types of carbon atoms. The ^{13}C NMR spectrum of $La_2@D_{5h}$-C_{80} exhibited six carbon signals (see Figure S2), thus providing the first evidence for the identification of the second isomer as $La_2@D_{5h}$-C_{80}. Subsequently, $La_2@D_{5h}$-C_{80} was reacted with **1** (see Figure 1) to examine its reactivity. Several new peaks were observed in the HPLC chromatogram after the reaction. Nevertheless, one dominant product **3** was obtained by a preparative HPLC technique using a Buckyprep column. The MALDI-TOF mass spectrum of **3** displayed a molecular ion peak at m/z 1470, corresponding to the rational formula of the triazinyl radical coupled $La_2@D_{5h}$-C_{80}, $La_2@D_{5h}$-C_{80}–$C_3N_3Ph_2$.

Compound **3** was also characterized by single-crystal XRD, though the final R value was relatively high owing to the low quality of the crystals. Similar to the case of **2**, the carbon cage is disordered. There are two overlapping orientations of the cage with refined occupancies of 0.64 and 0.36. In addition, there are eight lanthanum sites with occupancies ranging from 0.03 to 0.54. Nevertheless, it was apparent that the triazinyl radical was connected to one of the carbon atoms shared by one pentagon and two hexagon rings via a single bond, as shown in Figure 4.

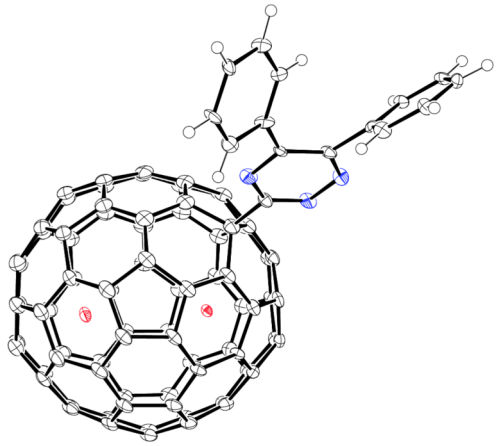

Figure 4. ORTEP drawing of **3** with thermal ellipsoids shown at the 50% probability level for 90 K. Solvate molecules are omitted for clarity. Only the major lanthanum sites and the major cage orientation are shown.

The paramagnetic character of **3** was clarified by electronic absorption and EPR spectroscopy. The broad absorption bands over the near-IR region down to 1300 nm in the electronic absorption spectrum of **3** indicate the possession of the paramagnetic nature (see Figure 5a). In addition, the EPR spectrum of **3**, shown in Figure 5b, resembles those of $La_2@I_h$-C_{80} anion and **2**. The observed spectrum is reproduced by the simulation using the parameters: $S = 1/2$, $g = 1.884$, $A(La_1) =$

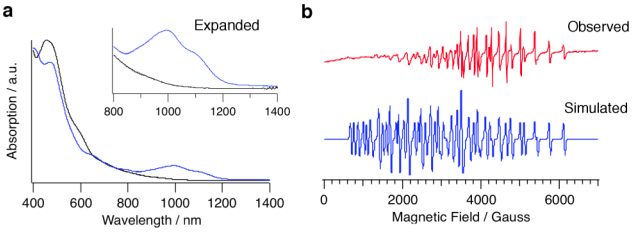

Figure 5. (a) Electronic absorption spectra of $La_2@D_{5h}$-C_{80} (black line) and **3** (blue line) in CS_2. (b) Observed (red line) and simulated (blue line) X-band EPR spectra of **3** in CS_2 observed at room temperature.

DOI: 10.1021/ja509956y
J. Am. Chem. Soc. 2015, 137, 232–238

$A(La_2)$ = 36.5 mT, ΔH_{pp} = 5 mT. The simulation again suggests a large, and identical, spin density is associated with each La atom. Although the two La atoms are found at nonequivalent sites in the crystal structure, the mobility of the lanthanum ions in the cage averages their individual environments. The spectrum of **3** is similar to that of **2**. The equally spaced hyperfine structure at the higher magnetic field never fits the simulation without using the isotropic parameters of $A(La_1) = A(La_2)$ = 36.5 mT.

Reactivity of the Radical 2. The chemical reactivity of **2** was tested to assess whether the internally localized radical center can couple further with another radical (Figure 6).

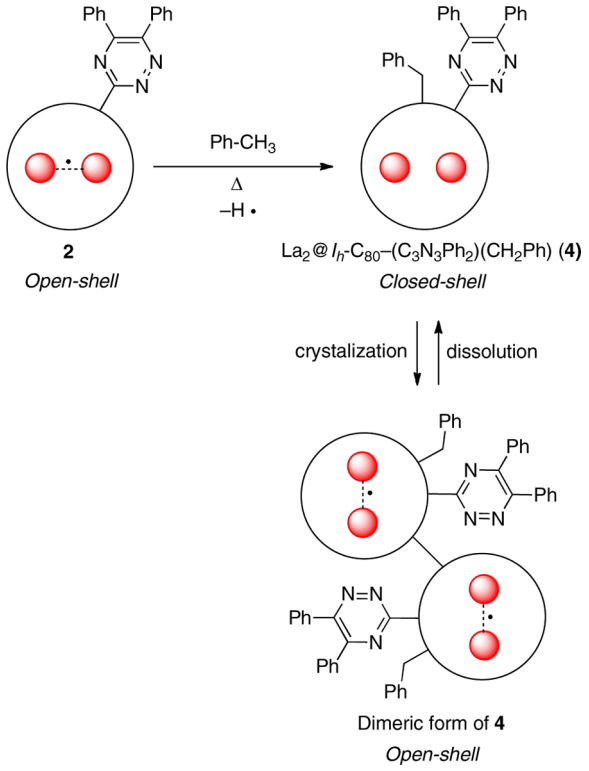

Figure 6. Reaction of **2** with toluene.

Heating of the mixture of **2** and an excess of toluene in 1,2-DCB yielded at least three products, among which the main product (**4**) was successfully purified using preparative HPLC (Figure S6). The MALDI-TOF mass spectrum of **4** displayed a molecular ion peak at m/z 1561, suggesting mono-addition of a benzyl radical to **2**. The asymmetric unit of **4** is $La_2@I_h$-C_{80}–$(C_3N_3Ph_2)(CH_2Ph)$. In fact, no EPR spectrum could be observed for **4** in CS_2, suggesting that **4** is diamagnetic in solution. Compared with that of **2**, the longest absorption band was red-shifted in the absorption spectrum of **4**, a situation that is consistent with its diamagnetic nature (see Figure 3a). The ^{1}H NMR spectrum of **4** exhibited an AB quartet comprised of doublets at 3.43 ($^2J_{H-H}$ =12.8 Hz) and 3.53 ($^2J_{H-H}$ =12.8 Hz) for the geminal hydrogen atoms of the benzyl group and signals for the phenyl group hydrogens at 7.11–7.64 ppm. These NMR signals are similar to those for a diamagnetic, dibenzylated derivative of $Sc_3N@I_h$-C_{80} reported by Dorn et al.[26]

The molecular structure of **4** was determined by single-crystal XRD. Crystals suitable for data collection were obtained from a solution of **4** in CS_2/n-hexane by slow evaporation of CS_2. Interestingly, the crystal structure shows that **4**, which possesses a triazinyl group and a benzyl group on the carbon cage, forms a dimer (i.e., $\{La_2@I_h$-C_{80}–$(C_3N_3Ph_2)(CH_2Ph)\}_2$) in the solid (Figure 7a). The intercage C–C distance between

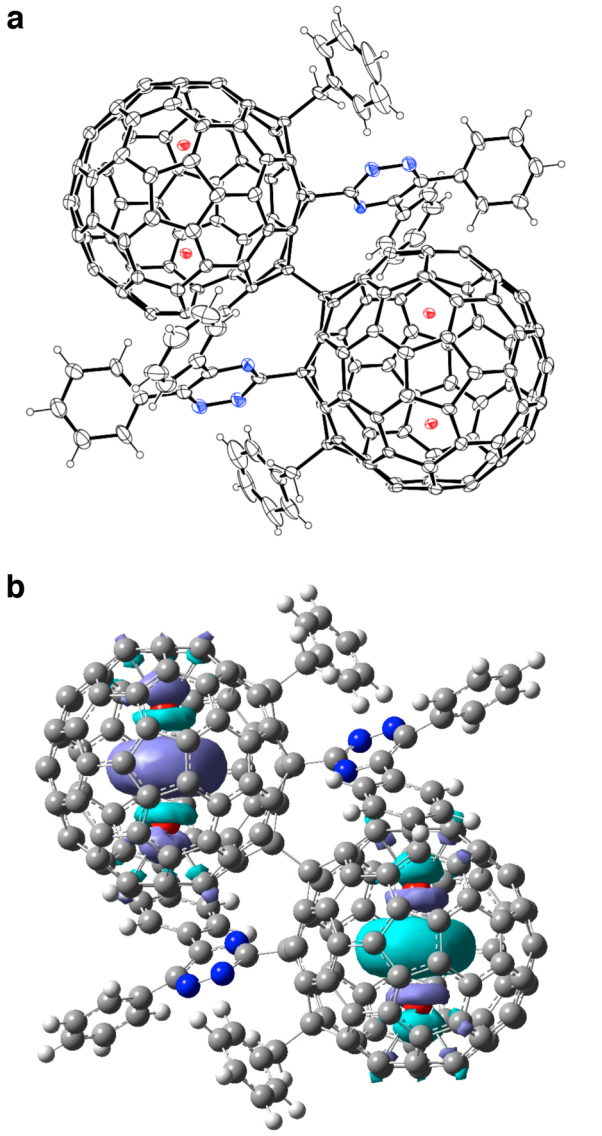

Figure 7. (a) ORTEP drawing of **4** as a dimeric form with thermal ellipsoids shown at the 30% probability level for 90 K. Solvate molecules and minor La sites are omitted for clarity. (b) The higher SOMO isoelectronic plot of the dimeric form of **4** in the triplet state calculated at the B3LYP/6-31G(d)~sdd level.

the two fullerene units is 1.587(14) Å, which is indicative of the formation of a C–C single bond between the two cages. The X-ray data revealed that the benzyl group was functionalized through the 1,7-position, whereas the dimer formation occurred at the carbon numbered as C11 (see Figure S14). Disorder involving the La atom locations is apparent in the cage interior. There is one prominent La pair with 0.89 site-occupancy. The other sites have small site-occupancies around 0.04 at 90 K. All the La sites are positioned along a band of 10 contiguous hexagons inside the cage.

DFT calculations show that the dimer formation is energetically favorable with an energy gain of 18.39 kcal mol^{-1} at the B3LYP/6-31G(d)~sdd level, in which the

DOI: 10.1021/ja509956y
J. Am. Chem. Soc. 2015, 137, 232–238

dimerization energy converts two monomers to the singlet state dimer. Therefore, we speculate that the dimer formation of **4** in crystals was thermodynamically controlled. Calculations at the B3LYP/6-31G(d)~sdd level also suggest that the triplet state is lower in energy by 22.81 kcal mol^{-1} than the singlet state. Therefore, the dimeric form of **4** should possess diradical character. The intercage C−C distance of the X-ray structure was also well reproduced by the DFT calculations (see Table S2). Figures 7b and S18 display the SOMO isoelectronic plots of the dimeric form of **4**. Apparently, two unpaired electrons occupy the internal La−La σ-bonding orbitals in the dimeric form of **4**. A broad signal was observed in the EPR spectrum of the crystal of **4**, as shown in Figure 8. On the other hand, the

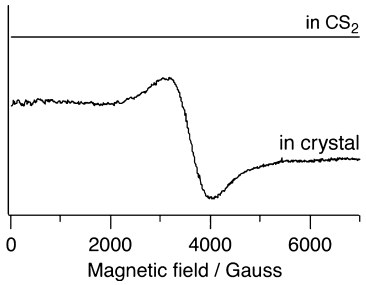

Figure 8. X-band EPR spectra of **4** measured in CS_2 (upper) and in crystal (lower).

signal disappeared when the crystal of **4** was dissolved in CS_2. The EPR-silent character of the solution indicates that **4** exists as a diamagnetic monomer in solution. The dimerization/dissociation process is reversible.[27]

CONCLUSION

We have shown that the radical reactions of two isomers of $La_2@C_{80}$ with 3-chloro-5,6-diphenyltriazine proceeded regioselectively to form isolable fullerenyl radicals. The molecular structures including the addition positions were determined using single-crystal XRD analyses. These results showed that the unpaired electrons are confined to the internal metal atoms in the fullerenyl radicals, where an endohedral $(La_2)^{5+}$ dimer is formed. In addition to this finding, the structure of the second isomer of $La_2@C_{80}$ was successfully identified to be $La_2@D_{5h}$-C_{80} for the first time. DFT calculations suggest that the formation of the fullerenyl radicals is not only thermodynamically but also kinetically controlled. The resulting fullerenyl radicals are stable in air despite their radical nature, showing that the internally isolated distribution of SOMOs is an effective means to stabilize the fullerenyl radicals. Furthermore, we have found that the fullerenyl radical **2** reacts with toluene under thermal conditions, to form a disubstituted derivative that is diamagnetic in solution. Remarkably, this benzylated derivative forms a paramagnetic dimer bearing diradical character when it is crystallized. Our results demonstrate the unique ability of endohedral fullerenes to stabilize an unpaired electron by localizing it on the La_2 unit inside the cage. This stabilization results in the formation of isolable radicals, **2** and **3**, and in the formation of dimeric **4**, where two cages couple and unpaired electrons are again placed on each La_2 unit.

EXPERIMENTAL SECTION

Preparation of $La_2@I_h$-C_{80} and $La_2@D_{5h}$-C_{80}. Both samples were obtained from the same synthetic and isolation procedure. The soot containing lanthanum EMFs was prepared using a composite anode that contains graphite and lanthanum hydroxide with the atomic ratio of La/C of 2.0%. The rod was subjected to an arc discharge as an anode under 150 Torr He pressure. The raw soot was collected and extracted with 1,2,4-trichlorobenzene for 15 h. The soluble fraction was injected into HPLC. Multistage HPLC separations were performed to give the purified products (see the Supporting Information for details). The purity of $La_2@I_h$-C_{80} and $La_2@D_{5h}$-C_{80} was examined with HPLC and mass spectrometry.

^{13}C NMR Data for $La_2@D_{5h}$-C_{80}. ^{13}C NMR (125 MHz, CS_2 (CD_3COCD_3 in capillary as lock solvent), 293 K) δ 159.93, 150.17, 144.02, 141.21, 137.14, 129.78 ppm.

Preparation of 2. A 1,2-DCB solution (1.3 mL) of $La_2@I_h$-C_{80} (1.0 mg, 0.81 μmol) and **1** (23 mg, 0.086 mmol) was degassed by freeze−pump−thaw cycles under reduced pressure. The mixture was heated at 200 °C for 12 h in a sealed Pyrex tube in the dark. After the reaction finished, the mixture was separated by preparative HPLC using a Buckyprep-M column (Φ20 × 250 mm, Nacalai Tesque Inc.) to afford pure **2** as a dark-brown solid. Yield, ca. 30% based on HPLC. MALDI-TOF MS (matrix = 1,1,4,4-tetraphenyl-1,3-butadiene): m/z 1470 ($[M]^+$).

Crystal Data for 2. Black plate, 0.28 × 0.17 × 0.04 mm, monoclinic, space group $P2_1/c$, a = 22.0705(16), b = 10.9858(8), c = 22.3824(17) Å, β = 114.202(4)°, V = 4949.9(6) $Å^3$, F_w = 1547.01, λ = 0.71073 Å, Z = 4, D_{calc} = 2.076 Mg m^{-3}, μ = 1.861 mm^{-1}, T = 90 K; 42201 reflections, 11306 unique reflections; 8486 with $I > 2\sigma(I)$; R_1 = 0.1638 [$I > 2\sigma(I)$], wR_2 = 0.4044 (all data), GOF (on F^2) = 1.171. The maximum residual electron density is 5.874 $eÅ^{-3}$. Crystallographic data have been deposited in the Cambridge Crystallographic Data Center (CCDC 1010739).

Preparation of 3. A 1,2-DCB solution (6.0 mL) of $La_2@D_{5h}$-C_{80} (2.5 mg, 2.2 μmol) and **1** (54 mg, 0.20 mmol) was degassed by freeze−pump−thaw cycles under reduced pressure. The mixture was heated at 200 °C for 24 h in a sealed Pyrex tube in the dark. After the reaction finished, the mixture was separated by preparative HPLC using a Buckyprep-M column (Φ20 × 250 mm, Nacalai Tesque Inc.) to afford pure **3** as a dark-brown solid. Yield, ca. 66% (based on HPLC). MALDI-TOF MS (matrix = 1,1,4,4-tetraphenyl-1,3-butadiene): m/z 1470 ($[M]^+$).

Crystal Data for 3. Black plate, 0.25 × 0.14 × 0.05 mm, monoclinic, space group $P2_1/c$, a = 23.242(11), b = 10.988(5), c = 22.219(10) Å, β = 112.174(5)°, V = 5255(4) $Å^3$, F_w = 1585.07, λ = 0.71073 Å, Z = 4, D_{calc} = 2.004 Mg m^{-3}, μ = 1.794 mm^{-1}, T = 90 K; 46953 reflections, 11803 unique reflections; 8020 with $I > 2\sigma(I)$; R_1 = 0.1652 [$I > 2\sigma(I)$], wR_2 = 0.3680 (all data), GOF (on F^2) = 1.176. The maximum residual electron density is 4.356 $eÅ^{-3}$. Crystallographic data have been deposited in the Cambridge Crystallographic Data Center (CCDC 1010738).

Preparation of 4. A 1,2-DCB solution (0.63 mL) of **2** (0.50 mg, 0.34 μmol) and toluene (0.63 mL) was degassed by freeze−pump−thaw cycles under reduced pressure. The mixture was heated at 110 °C for 24 h in a sealed Pyrex tube in the dark. After the reaction finished, the mixture was separated by preparative HPLC using a Buckyprep column (Φ20 × 250 mm, Nacalai Tesque Inc.) to afford pure **4** as a dark-brown solid. Yield, ca. 20% based on HPLC. ^1H NMR (400 MHz, CS_2/CD_2Cl_2 1:1) 3.43 (d, J = 12.8 Hz, 1H), 3.53 (d, J = 12.8 Hz, 1H), 7.11−7.64 (m, 20H). MALDI-TOF MS (matrix = 1,1,4,4-tetraphenyl-1,3-butadiene): m/z 1561 ($[M]^-$), 1470 ($[M - CH_2Ph]^-$).

Crystal Data for 4. Black plate, 0.20 × 0.06 × 0.04 mm, monoclinic, space group $P2_1/c$, a = 14.9753(4), b = 28.8596(7), c = 14.1361(4) Å, β = 111.710(2)°, V = 5676.0(3) $Å^3$, F_w = 3124.01, λ = 0.71073 Å, Z = 2, D_{calc} = 1.828 Mg m^{-3}, μ = 1.553 mm^{-1}, T = 90 K; 53122 reflections, 12974 unique reflections; 5715 with $I > 2\sigma(I)$; R_1 = 0.0578 [$I > 2\sigma(I)$], wR_2 = 0.1802 (all data), GOF (on F^2) = 0.993. The maximum residual electron density is 1.274 $eÅ^{-3}$. Crystallographic data have been deposited in the Cambridge Crystallographic Data Center (CCDC 1010737).

Theoretical Calculations. All calculations were carried out with the Gaussian 09 program package[28] using the B3LYP functional with

DOI: 10.1021/ja509956y
J. Am. Chem. Soc. 2015, 137, 232−238

the 6-31G(d) basis set for H, C, N atoms and the sdd basis for La (see the Supporting Information for details).

■ ASSOCIATED CONTENT

Supporting Information

Experimental details, additional spectroscopic and computational information, and CIF data. This materials is available free of charge via the Internet at http://pubs.acs.org.

■ AUTHOR INFORMATION

Corresponding Author

akasaka@tara.tsukuba.ac.jp

Notes

The authors declare no competing financial interest.

■ ACKNOWLEDGMENTS

Financial support from research on Innovative Areas (20108001, "π-Space"), Grants-in-Aid for Scientific Research (A) (202455006) and (B) (24350019), a Specially Promoted Research Grant (22000009) from the Ministry of Education, Culture, Sports, Science, and Technology of Japan, The Strategic Japanese−Spanish Cooperative Program funded by JST and MICINN, and the US NSF (Grant CHE-1305125) is gratefully acknowledged.

■ REFERENCES

(1) *Stable Radicals: Fundamentals and Applied Aspects of Odd-Electron Compounds*; Hicks, R. G., Ed.; John Wiley & Sons: Chichester, 2010.

(2) Tumanskii, B.; Kalina, O. *Radical Reaction of Fullerenes and their Derivatives*; Kluwer Academic Publishers: Dordrecht, 2001.

(3) Tzirakis, M. D.; Orfanopoulos, M. *Chem. Rev.* **2013**, *113*, 5262−5321.

(4) Krusic, P. J.; Wasserman, E.; Parkinson, B. A.; Malone, B.; Holler, E. R., Jr.; Keizer, P. N.; Morton, J. R.; Preston, K. F. *J. Am. Chem. Soc.* **1991**, *113*, 6274−6275.

(5) Morton, J. R.; Preston, K. F.; Krusic, P. J.; Hill, S. A.; Wasserman, E. *J. Phys. Chem.* **1992**, *96*, 3576−3578.

(6) Morton, J. R.; Preston, K. F.; Krusic, P. J.; Hill, S. A.; Wasserman, E. *J. Am. Chem. Soc.* **1992**, *114*, 5454−5456.

(7) Morton, J. R.; Preston, K. F.; Krusic, P. J.; Wasserman, E. *J. Chem. Soc., Perkin Trans. 2* **1992**, 1425−1429.

(8) Fagan, P. J.; Krusic, P. J.; Evans, D. H.; Lerke, S. A.; Johnson, E. *J. Am. Chem. Soc.* **1992**, *114*, 9697−9699.

(9) Fagan, P. J.; Krusic, P. J.; McEwen, C. N.; Lazar, J.; Parkert, D. H.; Herron, N.; Wasserman, E. *Science* **1993**, *262*, 404−407.

(10) Morton, J. R.; Negri, F.; Preston, K. F. *Acc. Chem. Res.* **1998**, *31*, 63−69.

(11) Koptyug, I. V.; Goloshevsky, A. G.; Zavarine, I. S.; Turro, N. J.; Krusic, P. J. *J. Phys. Chem. A* **2000**, *104*, 5726−5731.

(12) Haddon, R. C. *Nature* **1975**, *256*, 394−396.

(13) Morita, Y.; Suzuki, S.; Sato, K.; Takui, T. *Nat. Chem.* **2011**, *3*, 197−204.

(14) (a) Umeyama, T.; Imahori, H. *J. Mater. Chem. A* **2014**, *2*, 11545−11560. (b) Aguirre, J. C.; Ferreira, A.; Ding, H.; Jenekhe, S. A.; Kopidakis, N.; Asta, M.; Pilon, L.; Rubin, Y.; Tolbert, S. H.; Schwartz, B. J.; Dunn, B.; Ozolins, V. *J. Phys. Chem. C* **2014**, *118*, 19505−19523. (c) Gao, F.; Inganäs, O. *Phys. Chem. Chem. Phys.* **2014**, *16*, 20291−20304. (d) Wang, T.; Pearson, A. J.; Lidzey, D. G. *J. Mater. Chem. C* **2013**, *1*, 7266−7293. (e) Lin, Y.; Li, Y.; Zhan, X. *Chem. Soc. Rev.* **2012**, *41*, 4245−4272. (f) Li, C.-Z.; Yip, H.-L.; Jen, A. K.-Y. *J. Mater. Chem.* **2012**, *22*, 4161−4177. (g) Piliego, C.; Loi, M. A. H *J. Mater. Chem.* **2012**, *22*, 4141−4150. (h) Li, Y. *Acc. Chem. Res.* **2012**, *45*, 723−733. (i) Matsuo, Y. *Chem. Lett.* **2012**, *41*, 754−759. (j) Guldi, D. M.; Sgobba, V. *Chem. Commun.* **2011**, *47*, 606−610. (k) Walker, B.; Kim, C.; Nguyen, T.-Q. *Chem. Mater.* **2011**, *23*, 470−482. (l) Brabec, C. J.; Gowrisanker, S.; Halls, J. J. M.; Laird, D.; Jia, S.; Williams, S. P. *Adv. Mater.* **2010**, *22*, 3839−3856. (m) Liang, Y.; Yu, L. *Acc. Chem. Res.* **2010**, *43*, 1227−1236. (n) Delgado, J. L.; Bouit, P.-A.; Filippone, S.; Herranz, M. A.; Martín, N. *Chem. Commun.* **2010**, *46*, 4853−4865. (o) Roncali, J. *Acc. Chem. Res.* **2009**, *42*, 1719−1730. (p) Peet, J.; Heeger, A. J.; Bazan, G. C. *Acc. Chem. Res.* **2009**, *42*, 1700−1708. (q) Chen, L.-M.; Hong, Z.; Li, G.; Yang, Y. *Adv. Mater.* **2009**, *21*, 1434−1449. (r) Dennler, G.; Scharber, M. C.; Brabec, C. J. *Adv. Mater.* **2009**, *21*, 1323−1338. (s) Thompson, B. C.; Fréchet, M. J. *Angew. Chem., Int. Ed.* **2008**, *47*, 58−77. (t) Li, G.; Shrotriya, V.; Huang, J.; Yang, Y. *J. Mater. Chem.* **2007**, *17*, 3126−3140. (u) Günes, S.; Neugebauer, H.; Sariciftci, N. S. *Chem. Rev.* **2007**, *107*, 1324−1338. (v) Hoppe, H.; Sariciftci, N. S. *J. Mater. Chem.* **2006**, *16*, 45−61. (w) Hummelen, J. C.; Yu, G.; Gao, J.; Wudl, F.; Heeger, A. J. *Science* **1995**, *270*, 1789−1791.

(15) Abe, Y.; Tanaka, H.; Guo, Y.; Matsuo, Y.; Nakamura, E. *J. Am. Chem. Soc.* **2014**, *136*, 3366−3369.

(16) *Endofullerenes: A New Family of Carbon Clusters*; Akasaka, T., Nagase, S., Eds.; Kluwer Academic Publishers: Dordrecht, 2002.

(17) *Chemistry of Nanocarbons*; Akasaka, T., Wudl, F., Nagase, S., Eds.; John Wiley & Sons: Chichester, 2010.

(18) Popov, A. A.; Yang, S.; Dunsch, L. *Chem. Rev.* **2013**, *113*, 5989−6113.

(19) Zhang, Y.; Popov, A. A. *Organometallics* **2014**, *33*, 4537−4549.

(20) Suzuki, T.; Maruyama, Y.; Kato, T.; Kikuchi, K.; Nakao, Y.; Achiba, Y.; Kobayashi, K.; Nagase, S. *Angew. Chem., Int. Ed. Engl.* **1995**, *34*, 1094−1096.

(21) Yamada, M.; Slanina, Z.; Mizorogi, N.; Muranaka, A.; Maeda, Y.; Nagase, S.; Akasaka, T.; Kobayashi, N. *Phys. Chem. Chem. Phys.* **2013**, *15*, 3593−3601.

(22) Kato, T. *J. Mol. Struct.* **2007**, *838*, 84−88.

(23) Tsuchiya, T.; Wielopolski, M.; Sakuma, N.; Mizorogi, N.; Akasaka, T.; Kato, T.; Guldi, D. M.; Nagase, S. *J. Am. Chem. Soc.* **2011**, *133*, 13280−13283.

(24) In a related work, dimetallic endohedral heterofullerenes M_2@$C_{79}N$ (M = Y, Tb, and Gd) have been prepared and isolated. In these species, unpaired spin density is localized on the internal diatomic metal dimer; See: (a) Fu, W.; Zhang, J.; Fuhrer, T.; Champion, H.; Furukawa, K.; Kato, T.; Mahaney, J. E.; Burke, B. G.; Williams, K. A.; Walker, K.; Dixon, C.; Ge, J.; Shu, C.; Harich, K.; Dorn, H. C. *J. Am. Chem. Soc.* **2011**, *133*, 9741−9750. (b) Zuo, T.; Xu, L.; Beavers, C. M.; Olmstead, M. M.; Fu, W.; Crawford, T. D.; Balch, A. L.; Dorn, H. C. *J. Am. Chem. Soc.* **2008**, *130*, 12992−12997.

(25) Yamamoto, K.; Ishiguro, T.; Sakurai, K.; Funasaka, H.; Akasaka, T. In *Fullerenes: Recent Advances in the Chemistry and Physics of Fullerenes and Related Materials*; The Electrochemical Society: Pennington, NJ, 1997; Vol. *5*, pp 743−753.

(26) Shu, C.; Slebodnick, C.; Xu, L.; Champion, H.; Fuhrer, T.; Cai, T.; Reid, J. E.; Fu, W.; Harich, K.; Dorn, H. C.; Gibson, H. C. *J. Am. Chem. Soc.* **2008**, *130*, 17755−17760.

(27) In a related work, Poluektov et al. have demonstrated that fullerene heterodimers exhibit different conformations in solution and in solid films that change the fullerene's electronic coupling. In a covalently linked C_{60}−C_{70} heterodimer in blend with the polymer PCDTBT (poly[*N*-(1-octylnonyl)-2,7-carbazole]-*alt*-5,5-[4′,7′-di(-thien-2-yl)-2′,1′,3′-benzothiadiazole]), upon optical excitation of polymer:heterodimer solid films, the unpaired electron is shared between C_{60} and C_{70} cages. In contrast, the electron is localized on one half of the dimer in solution; see: Poluektov, O. G.; Nikias, J.; Mardis, K. L.; Beaupre, S.; Leclerc, M.; Villegas, C.; Erten-Ela, S.; Delgado, J. L.; Martin, N.; Sperlich, A.; Dyakonov, V. *Adv. Energy Mater.* **2014**, *4*, 1301517.

(28) Frisch, M. J.; Trucks, G. W.; Schlegel, H. B.; Scuseria, G. E.; Robb, M. A.; Cheeseman, J. R.; Scalmani, G.; Barone, V.; Mennucci, B.; Petersson, G. A.; Nakatsuji, H.; Caricato, M.; Li, X.; Hratchian, H. P.; Izmaylov, A. F.; Bloino, J.; Zheng, G.; Sonnenberg, J. L.; Hada, M.; Ehara, M.; Toyota, K.; Fukuda, R.; Hasegawa, J.; Ishida, M.; Nakajima, T.; Honda, Y.; Kitao, O.; Nakai, H.; Vreven, T.; Montgomery, J. A., Jr.; Peralta, J. E.; Ogliaro, F.; Bearpark, M.; Heyd, J. J.; Brothers, E.; Kudin, K. N.; Staroverov, V. N.; Kobayashi, R.; Normand, J.; Raghavachari, K.;

DOI: 10.1021/ja509956y
J. Am. Chem. Soc. 2015, 137, 232−238

Rendell, A.; Burant, J. C.; Iyengar, S. S.; Tomasi, J.; Cossi, M.; Rega, N.; Millam, M. J.; Klene, M.; Knox, J. E.; Cross, J. B.; Bakken, V.; Adamo, C.; Jaramillo, J.; Gomperts, R.; Stratmann, R. E.; Yazyev, O.; Austin, A. J.; Cammi, R.; Pomelli, C.; Ochterski, J. W.; Martin, R. L.; Morokuma, K.; Zakrzewski, V. G.; Voth, G. A.; Salvador, P.; Dannenberg, J. J.; Dapprich, S.; Daniels, A. D.; Farkas, Ö.; Foresman, J. B.; Ortiz, J. V.; Cioslowski, J.; Fox, D. J.*Gaussian 09*, revision A.02; Gaussian, Inc.: Wallingford, CT, 2009.

DOI: 10.1021/ja509956y
J. Am. Chem. Soc. 2015, 137, 232−238